Generation and Validation of Digital Elevation Model Using RISAT-1 SAR Interferometry

Ritesh Agrawal
Space Applications Centre / ISRO, Ahmedabad
Email: ritesh_agrawal@sac.isro.gov.in

(Received: 17 November 2022; in final form 31 August 2023)

DOI: *https://doi.org/10.58825/jog.2023.17.2.6*

Abstract: SAR Interferometry is one of the techniques used for generating three-dimensional information about the Earth's surface, which converts the absolute interferometric phase data of complex radar signal into topographic information. The prime objective of the study was to explore the potential of the RISAT-1 data for interferometric analysis. In this study, an attempt has made to generate the DEM of the part of Bharatpur region, Rajasthan using InSAR techniques using FFT based instead of the conventional approach due to non-availability of precise orbits. The analysis was carried out using FRS-1 data of 3 m resolution and 25 km swath corresponding to 21 February 2015 and 18 March 2015 having temporal separation of 25 days. The accuracy assessment of the generated DEM was compared with the extracted reference elevation information over 52 points from the Cartosat-1 DEM. The accuracy of the Generated DEM observed as 11.8 m and mean error of 2.3 m.

Keywords: RISAT-1, FRS, InSAR, Validation, Standard Deviation

1. Introduction

After the availability of initial Space-borne system, the generation of DEM performed using optical imagery and photogrammetric techniques (Crosetto and Aragues, 1999). The globally available elevation datasets cannot be used for the assessment of the local scale processes and on their impacts. The vertical error in the globally DEM datasets is the orders of magnitude higher than the magnitude at the estimate of the local level, such as in the case of river gradients, where the variation is much smaller than the vertical error. Urban flooding (Xu et.al, 2021; Jain et. al 2016) and 3-D city modelling (sharma et.al, 2016) is one of the examples where the precise DEM is more importance, which requires high resolution and accurate terrain. (Schumann & Bates, 2018). With the advancement in technology, Spaceborne imaging Synthetic Aperture radar (SAR) data gained and demonstrated high potential in generation of digital elevation model (DEM) of land surfaces (Mercer 1995; Bamler 1999; Das et al. 2014, Agrawal. et al., 2018). SAR datasets have two different approach for DEM generation (Gelautzet al, 2003). The radargrammetric approach works similar to photogrammetric approach using SAR amplitude image in place of optical image (Gelautz et al, 2003, Agrawal et al., 2018). The interferometric approach utilizes the phase information of the SAR image instead of the amplitude information for the generation of the DEM (Das et al. 2014, Abdelfattah and Nicolas, 2002, Zhouet al, 2005).
Two images from the coherent sources of the same region are required to form a phase difference images called as interferrogram (Zhou et al., 2009). The all-weather capability of techniques makes it powerful and cost effective data acquisition over a larger area (Zhou et al, 2005). The first InSAR results published by Goldstein et al. (1988) from the SEASAT L-band SAR data. In subsequent years, the ERS tandem mission provided a unique opportunity for the generation of the high-resolution DEM using repeat track interferometry. (Eldhuset et. al., 2003). Studies have demonstrated the potential of the interferometric technique to produce high-resolution topographic maps with relative height errors of 5m using repeat pass ERS imagery (Rufino, 1998, Eldhuset et. al., 2003, Jayaprasad et al, 2008, Shipping 2000). The standard approach for the generation of the DEM using InSAR includes image registration, interferogram calculation and filtering, phase unwrapping, elevation computation, and geocoding (Zhou et. Al, 2012; Geymen 2014), in which flat-earth removal has to rely on accurate orbital modeling to avoid long wavelength errors (Francis, 2006). The imaging quality, spatial and temporal baseline and atmospheric artifacts influence the accuracy of DEM. InSAR data processing also influence the DEM accuracy such as phase unwrapping, trends and planimetric errors. The image selection was carried out using baseline length and the minimization of the time-period of image acquisition to avoid baseline and temporal decorrelation (Arora and Patel, 2009).

RISAT-1 Synthetic Aperture Radar (SAR) is India's first indigenous, active, antenna-based microwave radar sensor in space, which was launched on 26 April 2012 from SDSC, SHAR, by Indian Space Research Organization (ISRO) (Valarmathi et al, 2013, Mahadevan et al, 2013). The spacecraft is 3-axis stabilized operating from an altitude of 536 km in sun synchronous orbit (Misra et al, 2013). It carrying a multi-mode Synthetic Aperture Radar (SAR) system provides complementary imaging capability in C-band with variety of resolution and swath requirements (Mahadevan et al, 2013). The resolutions from 3 to 50 m achieved with swath ranging from 25 to 223 km. In all the imaging modes, a novel polarimetry mode called circular or hybrid polarimetry also imagined (Misra et.al,2013). FRS-1 is a Stripmap mode while as MRS, CRS and FRS-2 are the ScanSAR-imaging mode.

This paper deals with generation of the DEM using repeat pass interferometry using FRS-1 Stripmap imaging mode

from the RISAT-1 satellite data. InSAR processing carried out using RH polarization from the circular polarimetric data. The datasets selected by keeping the minimum temporal and optimum baseline.

2. Study Area

Bharatpur district, Rajasthan covers an area of 5044.1 Km^2 and located between 26°40' and 27°50' latitude and 76°53' and 77°45'. The city of Bharatpur is popularly known as eastern gateway of Rajasthan. The city is enclosed between Gurgaon, Mathura, Agra, Dholpur, Dausa and Alwar. It is drained by three seasonal rivers viz., Gambhir River, tributaries of the Yamuna River, Ban Ganga River and Rooparel River. Limited availability of water resources confined the agriculture into traditional kharif cultivation and rabi cultivation is prevalent where irrigation facilities are available.

3. Data used

The RISAT-1 data has very limited datasets for the interferometric analysis due to less and non-systematic coverage of FRS-1 and the acquisition has limited data availability in terms of the similar geometry and baseline requirement. The data is selected from the pool of the FRS datasets by making the criteria having temporal separation of less than 2 month and variation in the look angle should be less than 0.2 deg. The FRS-1 Stripmap mode of RISAT-1 data (Table 1) is used in this study. InSAR analysis of data acquired on 21February and 18March of 2015 carried out having a time difference of 25 days (figure 1) is carried out.

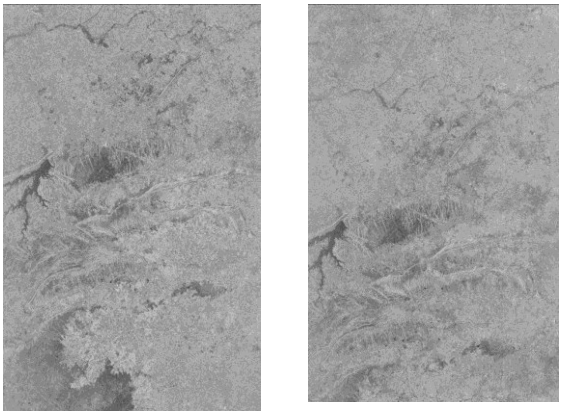

Figure 1. a) Master image (21st February), b) Slave image (18th march)

4. Methodology

The processing of SAR interferometric data is a complex issue. Based on the quality of the data sets, the performance of each single processing step has its influence on the final product. The basic steps involved in the derivation of topographic information from SAR images are shown in figure 2. The InSAR processing steps involves data importing, Orbit modelling, image co-registration, interferrogram generation, phase unwrapping to DEM generation. The precise orbital data plays an important role in the image co-registration error and flat earth correction and inaccurate orbital information can lead to misregistration of the image and inclusion of long wavelength error. In this study FFT based approach is used instead of the orbital based process to avoid misregistration and inclusion of the long wavelength error.

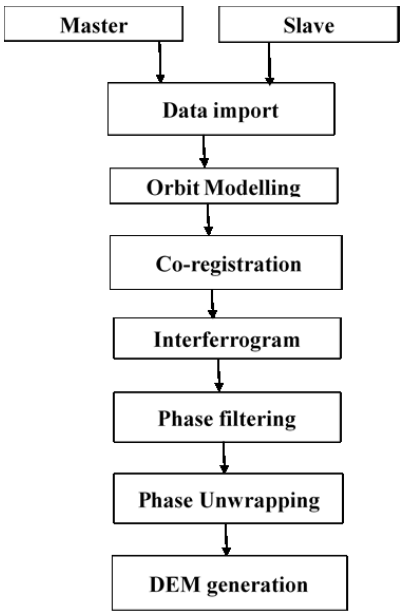

Figure 2. InSAR processing for the DEM generation.

5. Orbit Modelling

Importing of the data involves the importing of the SLC image along with the sensor parametrs, Image geometry parameters, orbital parameters along with the geolocational information of the scene centre and its extents. The extracted orbital information available in ECI co-ordinate system in RISAT-1 needs its conversion in ECEF co- ordinate system as shown in figure 3.

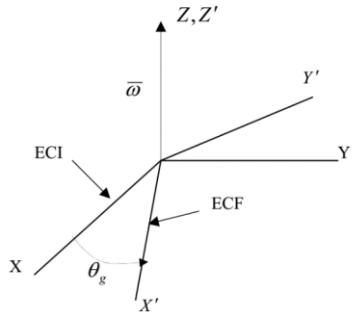

Figure 3. Conversion of ECI to ECF co-ordinate system

Since the state vectors consists of position and velocity,it is more appropriate to represent the trajectory as function of time so that the velocity will be the time derivative of the position; in this approach, the 2nd degree of polynomial takes the form as below:

$$X(t) = a_{x0} + a_{x1}.t + a_{x2}.t^2 \quad (1)$$
$$Y(t) = a_{y0} + a_{y1}.t + a_{y2}.t^2 \quad (2)$$
$$Z(t) = a_{z0} + a_{z1}.t + a_{z2}.t^2 \quad (3)$$

5.1. Image co-registration

Image co-registration is one of the key step for the interferometric processing. Variation in viewing geometry

of satellite from two parallel orbits cause small shift in one image with respect to other image. Image co-registration performs the geometrical alignment of the two SAR images covering same region. Image registration is performed in two steps as 1) coarse co-registration and 2) Fine co-registration.

The coarse co-registration computes the offset using orbital parameter by considering the centre co-ordinate of the master and estimate its location in the image grid for the master and slave image and its difference is considered the initial offset, which is further used for the estimation of the fine co-registration process.

Due to the unavailability of the precise ephemeris information of RISAT-1 orbital data, the computation of the offset between the two images may provide wrong estimation based on orbital parameter, which may yield in the wrong co-registration results in non-generation of interferogram. Estimation of the correct offsets computed by employing phase correlation (PC) approach, which utilizes the phase shift property of the Fourier transform to estimate large image offset. The purpose of the PC algorithm is to estimate the translation (Δx, Δy) between a pair of images sharing some common support: Let I1 (x, y) and I2 (x, y) be the images, then their common support satisfies.

$$I1\ (x + \Delta x, y + \Delta y) = I2\ (x, y) \quad (4)$$

The equation can be transformed in the FFT domain as

$$\widehat{I_1}(\omega_x, \omega_y) e^{j(\omega_x \Delta x + \omega_y \Delta y)} = \widehat{I_2}(\omega_x, \omega_y) \quad (5)$$

$$\frac{\widehat{I_2}(\omega_x, \omega_y)}{\widehat{I_1}(\omega_x, \omega_y)} = e^{j(\omega_x \Delta x + \omega_y \Delta y)} \quad (6)$$

The translation (Δx, Δy) can estimated by taking the inverse FFT

$$Corr\ (x, y) \triangleq \mathfrak{F}^{-1}\left\{e^{j(\omega_x \Delta x + \omega_y \Delta y)}\right\} = \delta(x - \Delta x, y - \Delta y) \quad (7)$$

Therefore, the translation values one estimated by maximum correlation in the image location:

$$(x, y) = arg\left\{\max_{(\tilde{x}, \tilde{y})} \{Corr\ (\tilde{x}, \tilde{y})\}\right\} \quad (8)$$

The fine co-registration process performs sub pixel level registrations. This process involves the selection of the multiple window in x and y direction within master image and corresponding smaller image segments selected in slave image over same locations. A search for the proper two-dimensional shift conducted using the correlation coefficient as the measure of goodness. In the oversampled image and the final image offset is estimated by the under sampled of the image offset with the same factors. The estimated offset parameters from the multiple windows modeled in the affine transformation model are given by the equations and used for the resampling of the slave image.

$X=\alpha_{00}+ \alpha_{10}X+ \alpha_{01}Y+ \alpha_{11}XY$
$Y=\beta_{00}+ \beta_{10}Y+ \beta_{01}X+ \beta_{11}XY$

5.2 Interferogram

Interferogram is defined as the product of the complex SAR values of a slave image and the complex conjugate of a master image. Flattening of the interferogram is carried out to remove the azimuth and range phase trends expected for a smooth curved Earth (Ellipsoid, height constant) from the interferogram.Adaptive filtering is carried out to reduce the phase noise in the flattened interferogram and thereby reducing the number of residues. The program reads the complex valued interferogram and filters the interferogram. The boxcar filter is applied for filtering the interferrogram to eliminate the noise present in the fringes. The filtered interferrogram is shown in Figure 4.

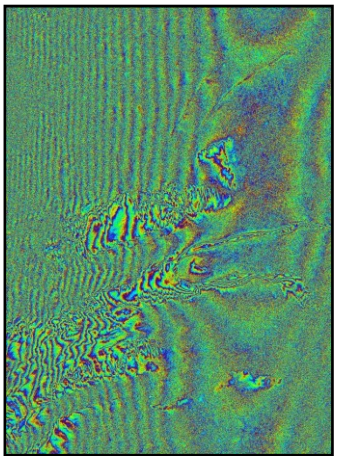

Figure 4. Filtered interferogram

$$R_i = \left\{\begin{matrix} \frac{1}{w}\sum_{j=0}^{w-1} A_{i+j-w/2} & if\ \frac{w-1}{2} \le i \le N - \frac{w+1}{2} \\ A_i \quad Otherwise \end{matrix}\right\} \quad (9)$$

5.3 DEM generation

For the computation of the absolute phase from the interferrogram, there is need for the computation of correct integer number of phase cycles that needs to add to each phase measurement in order to obtain the correct slant range distance. The process of computation of such absolute phase in terms of addition of integer multiple of 2π, is referred to as phase unwrapping. Absolute phase together with the precision baseline is used to compute topographic heights.

$$d\phi = -\frac{4\pi B}{\lambda H}\cos(\alpha - \theta)\sin\theta\cos\theta dz \quad (10)$$

where,

$d\phi$ is change in phase difference corresponding to change in elevation (dz)

B is the baseline length; H is the flying height of the satellite

θ is look angle; α is the angle made by the baseline vector. The computed elevation information refers in the image geometry. Geocoding is a process, which converts the image geometry in the map geometry. Conversion of such process is called geocoding. Geocoding removes all the distortions (Local, Global) and provides the end user a distorted free image in map coordinates. InSAR geocoding provides topographic information (DEM) in the map geometry by resampling using bilinear interpolation techniques.

6. DEM validation

Accuracy assessment for the DEM is normally performed by its comparison with the available topography maps or by collecting the elevation data from the field. The Cartosat-1 10 m DEM used as a reference DEM in this study and elevation points were collected randomly with suitable spatial and as well as the topographical distributed.

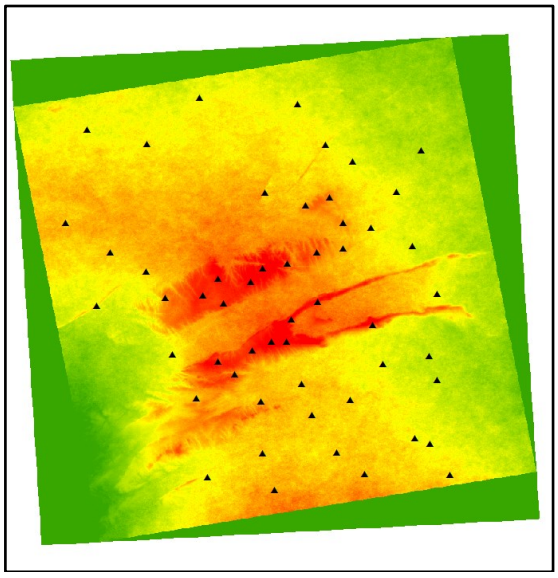

Figure 5. Points overlaid for accuracy assessment

These reference points used for the validation of the Generated DEM and the elevation value of the RISAT-1 Generated DEM compared with it. The figure 5 shows the distribution of control points used for evaluation of the DEM accuracy on the DEM generated by the RISAT-1 FRS datasets. Error analysis shows mean error of 2.23 m, while the RMSE observed is 11.8 m. The reference elevation values and the generated elevation values were compared at 52 points and shown as in the figure 6.

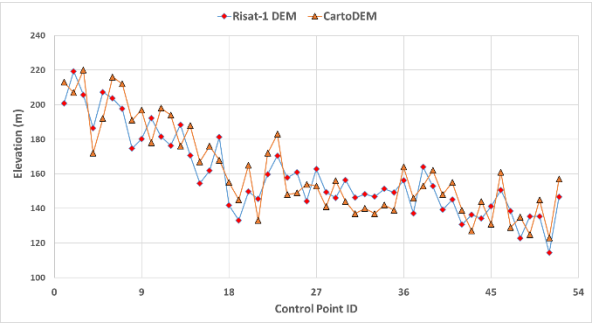

Figure 6. Comparison of the RISAT-1 DEM with CARTODEM

From the figure it is clear that the elevation values between the two DEMs are quite matching.

7. Conclusion

InSAR processing is described over the parts of the Bharatpur region, Rajashtan. An Improved FFT based co-registration approach used in this study instead of the conventional orbital-based approach, which is used for the avoid of the image mis-registration due to inaccuracy of the orbit. The study can perform the generation of the DEM even in the absence of the precise orbit. The accuracy of the generated DEM is compared with the Cartosat-1 DEM by comparing the elevation over 52 points. Error analysis shows mean error of 2.23 m, while the RMSE observed is 11.8 m. This study shows the potential of the FRS-1 datasets for the generation of the DEM with the required accuracy and the future Indian SAR satellite such as RISAT series FRS mode has capabilities for the interferometric applications.

Acknowledgement
Author express their sincere gratitude to Nilesh Desai, Director SAC. The author wishes sincerely thank the reviewers for their critical comments and suggestion for improving the quality of the paper

References

Abdelfattah R. and J.M. Nicolas (2002), Topographic SAR Interferometry Formulation for High-Precision DEM Generation, IEEE Transactions on Geoscience and Remote Sensing, 40(11), 2415- 2426

Agrawal R., A. Das and A.S. Rajawat (2018), Accuracy Assessment of Digital Elevation Model Generated by SAR Stereoscopic Technique Using COSMO-Skymed Data, Journal of the Indian Society of Remote Sensing, 46(10):1739–1747, doi: 10.1007/s12524-018-0835-6

Arora M.K. and V. Patel (2009), SAR Interferometry for DEM Generation, Geospatial world

Bamler R (1999). The SRTM mission—A worldwide 30 m resolution DEM from SAR interferometry in 11 days. In D. Fritsch & R. Spiller (Eds.), Photogrammetric week' 99 (pp. 145–154). Heidelberg, Germany: WichmannVerlag.

Crosetto M. and F. Aragues (1999), Radargrammetry and SAR Interferrometry for DEM generation: validation and data fusion, Proc. of the CEOS SAR Workshop, Toulouse, 26-29 October

Das A., R. Agrawal and S. Mohan (2014). Topographic correction of ALOS-PALSAR images using InSAR derived DEM. Geocarto International. https://doi.org/10.1080/10106049.2014.883436

Eldhuset K., P.H. Andersen, S. Hauge, E. Isaksson and D. Weydahl (2003), ERS tandem InSAR processing for DEM generation, glacier motion estimation and coherence analysis on Svalbard, International Journal of Remote Sensing, 24(7), 1415-1437

Francis I.O. (2006) InSAR Operational and Processing Steps for DEM Generation, Promoting Land Administration and Good Governance, 5th FIG Regional Conference Accra, Ghana, March 8-11, 2006

Gelautz M., P. Paillou, C.W. Chen, H.A. Zebker (2003), A Comparative Study of Radar Stereo And Interferometry For DEM Generation, Proc. of FRINGE 2003 Workshop, Frascati, Italy,1 – 5 December 2003

Geymen A. (2014) Digital elevation model (DEM) generation using the SARinterferometry technique, Arab J Geosci (2014) 7:827–837 DOI 10.1007/s12517-012-0811-3

Goldestein R.M., H.A. Zebker and C.L. Werner (1988), Satellite radar interferometry: Two-dimensional phase unwrapping. Radio Science, 23, 713–720

Jain G.V., R. Agrawal, R.J. Bhanderi, P. Jayaprasad, J.N. Patel, P.G. Agnihotriy and B.M. Samtani (2016) Estimation of sub-catchment area parameters for Storm Water Management Model (SWMM) using geo-informatics, Geocarto International 31 (4), 462-476

Jayaprasad P, B. Narender, S.K Pathan and Ajai (2008), Generation and Validation of DEM Using SAR Interferometry and Differential GPS Supported by Multispectral Optical Data, Journal of the Indian Society of Remote Sensing, 36, 343-352

Li S., H.P. Xu and Q. Zhang (2011), An Advanced DSS-SAR InSAR Terrain Height Estimation Approach Based on Baseline Decoupling, Progress In Electromagnetics Research, 119, 207-224

Mahadevan V., K. Prasad, D.S. Jain, S. Chowdhury, M. Pitchamani and N.M. Desai (2013), Ground segment for RISAT-1 SAR mission, Current Science, 104(4), 477-489

Mercer B. (1995). SAR technologies for topographic mapping. Photogrammetric week. Heidelberg, Germany: WichmannVerlag.

Misra T., S.S. Rana, N.M. Desai, D.B. Dave, R. Jyoti, R.K. Arora, C.V.N. Rao, B.V. Bakori, R. Neelakantan and J.G. Vachchan (2013), Synthetic Aperture Radar payload on-board RISAT-1: configuration, technology and performance, Current Science, 104(4), 446-461

Rufino G., A. Moccia and S. Esposito (1998), DEM Generation by Means of ERS Tandem Data, IEEE Transactions on Geoscience and Remote Sensing, 36 (6), 1905-1912

Schumann GJ-P and P.D. Bates (2018) The Need for a High-Accuracy, Open-Access Global DEM. Front. Earth Sci. 6:225. doi: 10.3389/feart.2018.00225

Sharma S.A., R. Agrawal and P. Jayaprasad (2016) Development of '3D city models' using IRS satellite data, Journal of the Indian Society of Remote Sensing 44,187-196

Shiping S., 2000, DEM Generation Using ERS-1/2 Interferometric SAR Data, In Proceeding of IGARSS2000, Honololu USA, 24-28 July 2000, 788-790

Valarmathi N, R.N. Tyagi, S.M. Kamath, B.T. Reddy, M.V. Ramana, V.V. Srinivasan, C. Dutta, N.V. Venketesh, Raveendranath, G.N. Babu, S. Prasad, R. Rajeev, P. Badagandi, S. Natarajan. J. Sudhakar, S.S. Rao and M.K. Reddy (2013), RISAT-1 spacecraft configuration: architecture, technology and performance, Current Science, 104(4), 462-471

Xu K., J. Fang, Y. Fang, Q. Sun, C. Wu and M. Liu, (2021) The Importance of Digital Elevation Model Selection in Flood Simulation and a Proposed Method to Reduce DEM Errors: A Case Study in Shanghai, Int J Disaster Risk Sci (2021) 12:890–902, DOI: 10.1007/s13753-021-00377-z

Zhou C., G.E. Linlin, E. Dongchen and H. Chang (2005), A Case Study of Using External DEM in InSAR DEM Generation, Geo-spatial Information Science, Volume 8, No. 1, 14-18

Zhou H., J. Zhang, L. Gong and X. Shang (2012) Comparison and Validation of Different DEM Data Derivedfrom InSAR, Procedia Environmental Sciences 12, 590 – 597

Zhou X., N. B. Chang and S. Li (2009), Applications of SAR Interferometry in Earth and Environmental Science Research, Sensors,9, 1876-1912; doi:10.3390/s9030187